Small-angle x-ray scattering of porous silicon at two different wavelengths



1998 J. Phys.: Condens. Matter 10 9969

(http://iopscience.iop.org/0953-8984/10/44/005)

J. Phys.: Condens. Matter **10** (1998) 9969–9974. Printed in the UK PII: S0953-8984(98)91908-7

# Small-angle x-ray scattering of porous silicon at two different wavelengths

S Mazumder†, D Sen†, P U M Sastry†, R Chitra†, A Sequeira† and K S Chandrasekaran‡

† Solid State Physics Division, Bhabha Atomic Research Centre, Trombay, Mumbai 400 085, India

‡ Solid State Electronics, Tata Institute of Fundamental Research, Colaba, Mumbai 400 005, India

Received 20 February 1998, in final form 29 June 1998

**Abstract.** A sample of lightly doped p-type porous silicon has been investigated by small-angle x-ray scattering (SAXS) at two different wavelengths (0.154 and 0.071 nm) of the probing radiation. The scattering profiles are found to have distinctly different functionality, independently indicating the importance of accounting for multiple-scattering effects. The extracted single-scattering profile can be explained in terms of mixed cylindrical and spherical pores, without recourse to fractal structures.

## 1. Introduction

Porous silicon (PS) is a technological material with potential for opto-electronic integration [1]. A detailed understanding of its pore structure is relevant to its light-emitting characteristics. The pertinent structure in PS can be accessed by small-angle x-ray scattering (SAXS) and there are a few reports [2–7] on systematic structural investigations on PS by means of SAXS.

Vezin *et al* [2, 3] investigated the effect of the doping level on the microstructure of p-type porous silicon. They found that in nondegenerate p-type PS, the pore structure is apparently a random distribution of spherical pores. In degenerately doped p-type silicon, the film consists of cylindrical voids with their axes perpendicular to the surface. They had also investigated PS layers with varying degrees of porosity on lightly p-doped wafers. Some of their experimental observations have been explained by invoking a mass fractal model of porous silicon. Goudeau *et al* [4, 5] investigated both lightly and heavily doped wafers. SAXS data for both lightly and heavily doped p-type samples were interpreted in terms of fractal structure and in terms of cylindrical pores for the lightly doped n-type sample. Binder *et al* [6, 7] in their more recent studies investigated both $p^-$- and $p^+$-doped PS. In the case of $p^-$ samples, the scattering profiles can be explained in terms of a bimodal distribution of spherical pores. For $p^+$-doped PS samples, they can be ascribed to the existence of cylindrical pores oriented perpendicularly to the surface. No fractal structure need be invoked to explain the data.

In all of the aforementioned work, the conclusions have been drawn under the single-scattering approximation [8]. Since the pores in the silicon matrix are strongly scattering (the scattering-length-density contrast being $1.97 \times 10^{-3}$ nm$^{-2}$), with some cylindrical pores

0953-8984/98/449969+06$19.50  

of lengths of the order of the thickness of the porous layer, and the typical porosity in the range 30–85%, we considered it important to check the validity of the single-scattering approximation by carrying out measurements at two different wavelengths on the same sample. Here we present the results obtained on lightly doped p-type porous silicon by SAXS experiments carried out at 0.154 and 0.071 nm respectively with Cu K$\alpha$ and Mo K$\alpha$ x-rays.

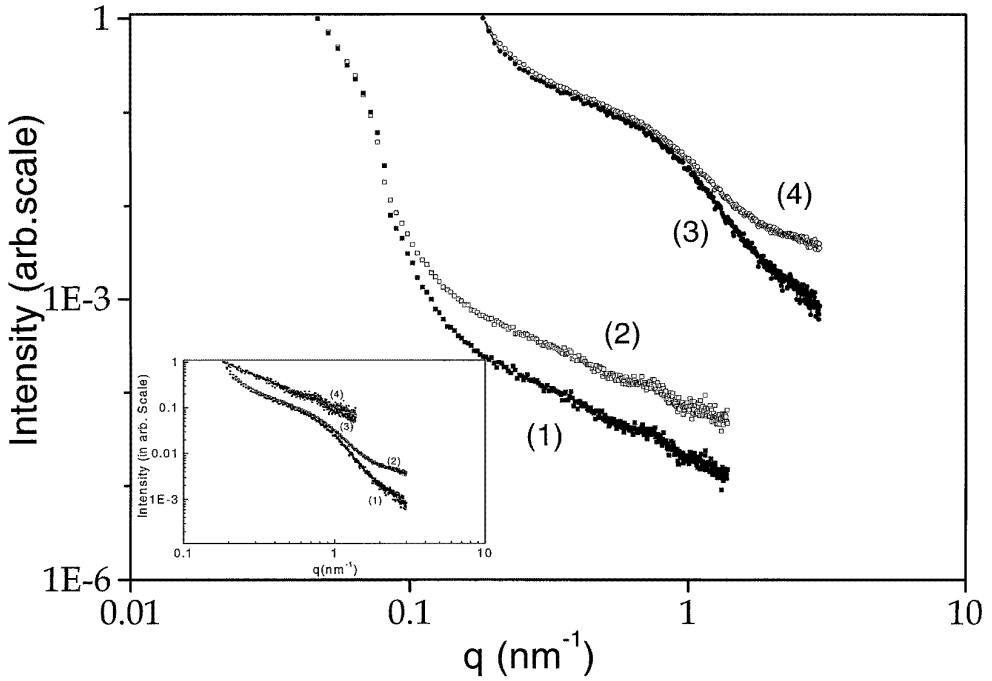


**Figure 1.** Raw and corrected collimation and transmission data on a porous layer sample 13.5 $\mu$m thick obtained using Mo K$\alpha$ and Cu K$\alpha$ radiation. Curves (2) and (4) correspond to raw data while curves (1) and (3) correspond to the corrected data. Cu K$\alpha$ radiation was used to record data set (2) while Mo K$\alpha$ radiation was used to record data set (4). $q$ represents the modulus of the wave-vector transfer for the small-angle scattering experiments. Over the $q$-range 2.615–2.986 nm$^{-1}$, curves (1) and (2) follow power laws, $\sim q^{-3.022}$ and $\sim q^{-1.393\,71}$, respectively. Over the $q$-range 1.214–1.385 nm$^{-1}$, curves (3) and (4) also follow power laws, $\sim q^{-1.15}$ and $\sim q^{-0.196}$, respectively.

The inset depicts normalized scattering profiles. The intensities of the individual scattering profiles are fixed at 1.0 for a $q$-value of 0.1852 nm$^{-1}$. Curves (2) and (4) correspond to raw data while curves (1) and (3) correspond to the corrected data. Cu K$\alpha$ radiation was used to record data set (2) while Mo K$\alpha$ radiation was used to record data set (4).

## 2. Experiment

### *2.1. Samples*

The porous silicon samples were prepared on p-type silicon wafers, (100) oriented, lightly boron doped and with a resistivity of 4–7 $\Omega$ cm. The wafers were 390 $\mu$m thick. An ohmic back-contact was provided by aluminium evaporation and sintering at 600 °C. The wafers were anodized in ethanol:HF 1:1 solution at a current density of 10 mA cm$^{-2}$. The

anodic reaction time was varied to obtain porous layers of different thicknesses. The typical formation rate of the porous Si was $\sim$0.45 $\mu$m min$^{-1}$.

### *2.2. SAXS experiments*

The SAXS measurements were carried out with a rotating-anode-based Rigaku SAXS goniometer, operated at 6–8 kW power, which is a three-slit system with Soller slits. The intensity was measured by a scintillation counter with a pulse height analyser for respective wavelengths of x-rays. Ni-filtered Cu K$\alpha$ and Zr-filtered Mo K$\alpha$ radiation were used as the incident x-ray sources. The scattered intensities were recorded as a function of $q$ ($=4\pi(\sin\theta)/\lambda$, $2\theta$ being the scattering angle and $\lambda$ the x-ray wavelength). The intensities were corrected for sample absorption and for the smearing effects of the collimating slits [10].

## 3. Data analysis

The raw measured and the corrected data obtained using Cu K$\alpha$ and Mo K$\alpha$ radiation are depicted in figure 1. The scattering data recorded using Mo K$\alpha$ radiation shows a distinct shoulder, while the data recorded with Cu K$\alpha$ radiation do not have that feature. Furthermore, the two profiles have distinctly different functionality. The inset of figure 1 depicts the wavelength dependence of the scattering profiles on a normalized scale to allow one to appreciate the distinct functionalities of the profiles. The intensities of the individual scattering profiles are fixed at 1.0 at $q = 0.1852$ nm$^{-1}$, the lowest $q$-value attained in the present experiment using Mo K$\alpha$ radiation. The Cu K$\alpha$ data for the range $q < 0.1852$ nm$^{-1}$ are not represented in the inset of figure 1.

It is important to note that in conventional SAS, where the single-scattering approximation holds good, variation of the sample thickness or wavelength does not change the functionality of the profile; i.e., the profiles are different as regards a scale factor only. Even from the very first observation of the dependence of the functionality of the scattering profile on the wavelength, it was concluded that the pores could be cylindrical in shape with the axes of the cylinders aligned with the incident beam direction. In such a situation, the scattering mean free path $L$ of the radiation takes the form

$$L = \frac{1}{\phi l \lambda^2 D^2} \tag{1}$$

where $\lambda$ is the wavelength of the probing radiation and $D$ is the scattering-length-density contrast, $l$ is the length of the capillary pores and $\phi$ is the packing fraction of the pores in the medium. Since the length of the capillary pores could be of the order of a micrometre we consider that the multiple-scattering effects will be quite significant. To give an example, for a 50% porous sample and cylindrical pores with length 1.0 $\mu$m,

$L = 21.73$ $\mu$m for Cu K$\alpha$ radiation ($\lambda = 0.154$ nm)

$L = 102.23$ $\mu$m for Mo K$\alpha$ radiation ($\lambda = 0.071$ nm).

So it is evident that for a sample with a porous layer thickness of 13.5 $\mu$m, it will be a gross error to treat the data under the single-scattering approximation, which is valid only for thicknesses $\leqslant L/10$ [9].

It is important to note that, for a spherical inhomogeneity of radius $R$, $L$ is given by

$$L = \frac{2}{3\phi R \lambda^2 D^2}. \tag{2}$$

So, if one is to observe an appreciable effect of multiple scattering, $R$ has to be $\geqslant 1.0$ $\mu$m.

To verify our assessment that the cylinders are oriented perpendicularly to surface, we tilted one of the samples and observed the profile changes, as shown in figure 2, with tilting. However, rotation of the sample in its own plane about the incident beam axis does not change the profile to any significant extent. We have estimated [9] the scattering mean free path $L$ of both probing radiations in the sample. The estimated $L$-values are $L = 38.352$ ($\pm 2.685$) $\mu$m for Mo K$\alpha$ radiation and $L = 8.157$ ($\pm 0.571$) $\mu$m for Cu K$\alpha$ radiation.

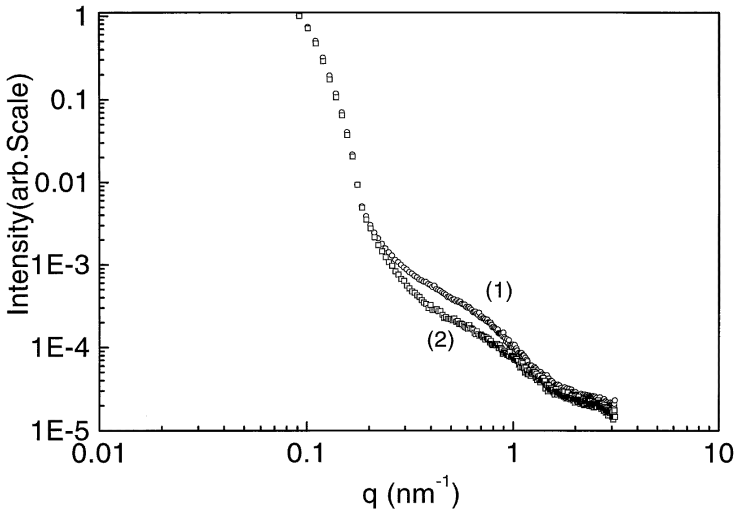


**Figure 2.** Scattering profiles of a sample with a porous layer 6.75 $\mu$m thick, recorded using Mo K$\alpha$ radiation before and after tilting the sample by about seven degrees. Curve (1) corresponds to the raw data recorded without tilting and curve (2) corresponds to the data recorded with tilting.

For 50% porosity, as measured by the gravimetric method, we estimate the length $l$ of the pores to be 2.664 ($\pm 0.186$) $\mu$m when the system is monodisperse. For a polydisperse system, 2.664 $\mu$m would correspond to $\langle l^2\rangle/\langle l\rangle$ assuming that all of the cylindrical pores are of uniform cross-section and that averaging is carried out with respect to the population distribution. However, for a system that is a mixture of cylindrical and spherical pores, 2.664 $\mu$m would correspond to $g\langle l^2\rangle/\langle l\rangle + (1-g)(3/2)\langle R^4\rangle/\langle R^3\rangle$ where $g$ denotes the population fraction of cylindrical pores.

The extracted [9] single-scattering profile is shown by curve (1) in figure 3. The profile has many shoulders at its tail due to either shape dispersion or the effects of interference between the pores. As the system is very dense, such interference effects occur at relatively high values of $q$. Over the $q$-range 2.26–3.06 nm$^{-1}$, the scattering profile follows a power law, $\sim q^{-2.934}$, which is close to the form $\sim q^{-3.022}$ observed in the case of the corrected profile of the sample recorded using Mo K$\alpha$ radiation. It is noteworthy that for cylindrical pores with the axes of the pores aligned with the incident beam, the expected power law is $\sim q^{-3}$ [11].

The form of the single-scattering profile can be explained by there being a mixture of differently shaped objects. We did model calculations with a mixture of spherical and cylindrical particles which also has the same features as are shown by curve (3) in figure 3.

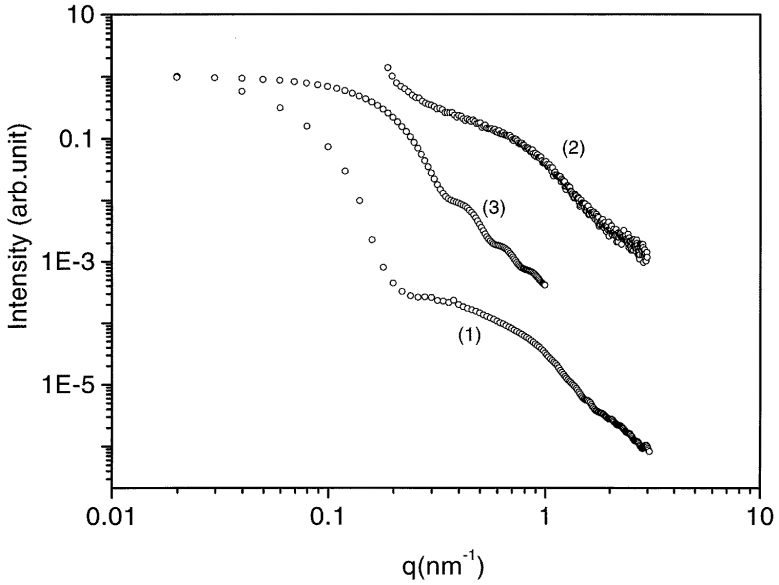


**Figure 3.** The estimated single-scattering profile, curve (1), compared with the recorded (using Mo K$\alpha$ radiation) scattering profile, curve (2), which is affected by multiple scattering. Curve (3) represents the scattering profile of a model system consisting of a mixture of cylindrical particles with radius 1.0 nm, length 100.0 nm and a square-wave dispersion of spherical particles with radii ranging between 5.0 and 15.0 nm.

Curve (3) in figure 3 is the outcome of a model calculation with a mixture of cylindrical particles of radius 1.0 nm, length 100.0 nm and a dispersion of spherical particles with radii ranging between 5 and 15 nm following a square-wave distribution. It was not found necessary to invoke fractal structure to explain the data.

The single-scattering profile has two distinct Guinier slopes, namely $-264.88$ nm$^2$ for the wave-vector range $\leqslant 0.16$ nm$^{-1}$ and $-2.96$ nm$^2$ for the wave-vector range 0.4–0.7 nm$^{-1}$. We interpret the first slope as due to some spherical particles and the second one as due to the radius of the cylindrical pores, which is estimated to be 3.44 nm. If the physical system is modelled as a mixture of polydisperse spherical particles and polydisperse cylindrical particles with dispersion only in length, then from the slope at the lower $q$-values we have $\langle R^8\rangle/\langle R^6\rangle = 1324.23$ nm$^2$.

The estimated single-scattering profile is best interpreted with a mixture of polydisperse spherical particles, curve (1) in figure 4, and polydisperse cylindrical particles, curve (2) in figure 4, with a fixed cross-sectional radius of 3.44 nm. The fit used constraints, namely

$$\langle R^8\rangle/\langle R^6\rangle = 1324.23 \text{ nm}^2$$
$$g\langle l^2\rangle/\langle l\rangle + (1-g)(3/2)\langle R^4\rangle/\langle R^3\rangle = 2.664\ \mu\text{m}$$

with $g$ found to be 0.845.

## 4. Conclusions

We conclude that the pores in lightly doped porous silicon have mixed shapes. The observed feature of the functionality varying with the wavelength is indicative of the presence of

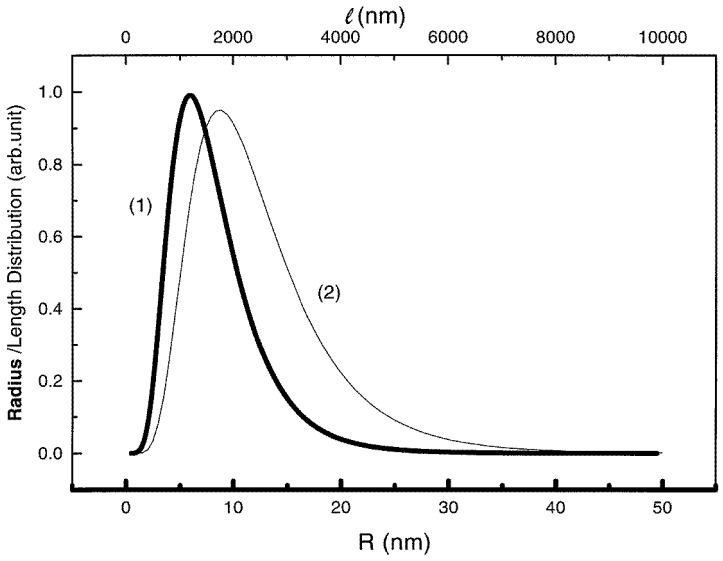


**Figure 4.** Curve (1) is the estimated radius distribution function, depicted by the thick line. The distribution has the following characteristics: $\langle R \rangle = 8.339$ nm, $\langle R^2 \rangle = 87.247$ nm$^2$ and the peak position is at 5.93 nm. Curve (2) is the estimated length distribution function. The scale of the $x$-axis relevant to this curve is indicated at the top of the frame. The distribution has the following characteristics: $\langle l \rangle = 2.4875$ $\mu$m, $\langle l^2 \rangle = 7836$ $\mu$m$^2$ and the peak position is at 1.745 $\mu$m.

cylindrical pores. Cylindrical pores have a broad distribution with a peak at a fraction of the porous layer thickness. However, some pores could be as long as half of the porous layer thickness. Multiple scattering has to be accounted for in explaining the structural features of porous silicon found by SAXS experiments. We do not need the assumption of fractal surfaces to explain the data.

## Acknowledgments

We thank Professor K L Narasimhan for useful discussions and A Deorukhkar and V Driver for their help in growing the samples.

## References

[1] Smith R L and Collins S D 1992 *J. Appl. Phys.* **71** R1–22
[2] Vezin V, Goudeau P, Naudon A, Herino A and Bomchil G 1991 *J. Appl. Crystallogr.* **24** 581–7
[3] Vezin V, Goudeau P, Naudon A, Halimaoui A and Bomchil G 1992 *Appl. Phys. Lett.* **60** 2625–7
[4] Goudeau P, Naudon A, Bomchil G and Herino R 1989 *J. Appl. Phys.* **66** 625–8
[5] Naudon A, Goudeau P, Halimaoui A, Labbert B and Bomchil G 1994 *J. Appl. Phys.* **75** 780–4
[6] Binder M, Edelmann T, Metzger T H, Mauckner G, Goerigk G and Peisl J 1996 *Thin Solid Films* **276** 65–8
[7] Binder M, Edelmann T, Metzger T H and Peisl J 1996 *Solid State Commun.* **100** 13–6
[8] Mazumder S and Sequeira A 1990 *Phys. Rev.* B **41** 6272–7
[9] Mazumder S, Jayaswal B and Sequeira A 1998 *Physica* B at press
[10] Schmidt P W and Hight R 1960 *Acta. Crystallogr.* **13** 480–3
[11] Porod G 1982 *Small-angle X-ray Scattering* ed O Glatter and O Kratky (London: Academic) p 17